Chapter 7

Elevated brain iron is independent from atrophy in Huntington's Disease

Eve M Dumas[1], Maarten J Versluis[2], Simon JA van den Bogaard[1], Matthias JP van Osch[2,3], Ellen P Hart[1], Willeke MC van Roon-Mom[4], Mark A van Buchem[2,3], Andrew G Webb[2,3], Jeroen van der Grond[3], Raymund AC Roos[1], on behalf of the TRACK-HD investigators

1. Department of Neurology, Leiden University Medical Center
2. CJ Gorter Center for High Field MRI, Department of Radiology, Leiden University Medical Center
3. Department of Radiology; Leiden University Medical Center
4. Department of Human Genetics; Leiden University Medical Center

Neuroimage (2012) 61(3): 558-64

Abstract

Increased iron in subcortical structures in patients with Huntington's Disease (HD) has been suggested as a causal factor of neuronal degeneration. The present study examines iron accumulation, measured using magnetic resonance imaging (MRI), in premanifest gene carriers and in early HD patients as compared to healthy controls. In total 27 early HD patients, 22 premanifest gene carriers and 25 healthy controls, from the Leiden site of the TRACK-HD study, underwent 3T MRI including high resolution 3D T_1- and T_2-weighted and asymmetric spin echo (ASE) sequences. Magnetic Field Correlation (MFC) maps of iron levels were constructed to assess magnetic field inhomogeneities and compared between groups in the caudate nucleus, putamen, globus pallidus, hippocampus, amygdala, accumbens nucleus, and thalamus. Subsequently the relationship of MFC value to volumetric data and disease state was examined. Higher MFC values were found in the caudate nucleus ($p<0.05$) and putamen ($p<0.005$) of early HD compared to controls and premanifest gene carriers. No differences in MFC were found between premanifest gene carriers and controls. MFC in the caudate nucleus and putamen is a predictor of disease state in HD. No correlation was found between the MFC value and volume of these subcortical structures. We conclude that Huntington's disease patients in the early stages of the disease, but not premanifest gene carriers, have higher iron concentrations in the caudate nucleus and putamen. We have demonstrated that the iron content of these structures relates to disease state in gene carriers, independently of the measured volume of these structures.

Introduction

Huntington's Disease (HD) is an autosomal dominant neurodegenerative disorder characterised by brain atrophy and clinical deterioration in the domains of motor function, cognition and behaviour. HD is caused by an expanded CAG repeat in the *HTT* gene on the short arm of chromosome 4. Genetic testing can be performed in those at risk, prior to disease onset, to ascertain that they carry the gene and will develop the disease in the future. Histological reports describe profound cellular structure deterioration of the putamen and caudate nucleus[1-3], as well as iron accumulation[4]. Autopsy brain tissue extractions confirmed these findings in end-stage patients by demonstrating increased absolute iron levels in these structures[5].

MRI has been shown to be a valuable tool for estimating iron levels in vivo[6;7]. Several MRI techniques have been used to assess the distribution of iron in the brain in normal aging[8-10] and in neurodegenerative diseases[11-14]. These include T_2 and T_2* mapping, as well as susceptibility weighted imaging (SWI). Each of these techniques is simple to perform, but have significant potential limitations. A confounding factor of both T_2- and T_2*-based imaging is that measurements are also affected by changes in the water content, associated for example with destructive brain processes[15], and can mask the changes in iron content[6;9;14;16;17]. Ex vivo histological staining of putamen samples from HD patients demonstrated elevated putamen iron levels[18] but there was little correlation to T_2-weighted imaging of these samples. To overcome these limitations T_2 can be measured at two different field strengths to remove the field independent contribution to T_2 changes. Because the T_2 value of water is relatively field strength independent[19], this method is a more sensitive measurement of iron content. However, scanning subjects on two different MRI systems is clinically impractical. MRI approaches based on changes in T_2* relaxation time have also been widely applied[16]. In addition to the sensitivity of the measurement to water content, a specific limitation of T_2* imaging techniques is that measurements are affected by local background sources of magnetic field inhomogeneities that cause signal loss unrelated to the internal iron content of the tissue[6]. SWI is a technique that provides an additional measure for detecting iron related changes by combining magnitude and phase data into a single image[20]. Because changes in the magnetic field also lead to changes in the MRI signal phase, it has been suggested as a more sensitive method for detecting neurodegenerative disease related iron changes[17]. However SWI is not a quantitative method and the limitations mentioned above for T_2* techniques are also true for SWI. Hence, the limitations posed by the above described methods demonstrates the need for further development and application of existing and new techniques[12].

The recently developed quantitative technique of magnetic field correlation (MFC) imaging has the potential to solve the limitations of previously applied MRI techniques in HD.

MFC is sensitive to spatially inhomogeneous magnetic fields, such as those generated by iron-rich regions. An advantage is that this technique is insensitive to changes in water concentration. For this reason MFC has previously been used to study increased iron concentrations in the basal ganglia in patients with aceruloplasminemia[21], patients with traumatic brain injury[22] and in patients with multiple sclerosis[23]. The relationship between the measured MFC values and magnetic field inhomogeneities is more direct compared to other relaxometry measurements, allowing for a clearer physical interpretation of MFC measurements[21;24]. Furthermore, MFC imaging can be implemented practically in a single short scan at one field strength.

Previous MRI studies have suggested that increased iron in the striatum could be a causal factor of the symptoms of HD[11;19]. Given that both prior to, and after, disease onset, brain changes in the form of volumetric reductions have been systematically reported[25-28], it is possible that iron levels change both in the premanifest and in the manifest stages of the disease. However, this hypothesis has only been examined previously in one group of premanifest gene carriers of HD[29]. It has been suggested that increases in iron could promote neurotoxicity through the induction of oxidative reactions[12;30]. A question still debated is whether these iron changes are causal or secondary factors of disease processes. With this current study we aim to determine at which disease stage iron accumulations increase in HD.

It remains unclear to what extent iron changes are independent of volume decreases in both the premanifest and manifest phases of the disease, or whether iron levels alter as a direct result of volumetric change[25;28;31]. Volume decreases may concentrate the iron that is already present, or alternatively more iron may accumulate as the disease progresses. It is important for our understanding of HD, as well as for future research, to differentiate between these pathophysiological mechanisms. For this reason, the second aim of this study is to examine and relate the potential iron changes to the amount of atrophy present in the related subcortical grey matters structures.

The current reports of iron in HD examined only a selection of the subcortical grey matter structures. However, recently atrophy has been demonstrated in seven major subcortical structures in the progressive stages of HD[27]. In this current study we investigate in both premanifest and early HD the extent to which elevated iron may be present. We hypothesize that iron concentrations will be higher in these subcortical grey matter structures in HD patients. Furthermore, we expect that iron may play a role in HD that is not explained by volumetric differences.

Material and Methods

Participants

Participants were recruited from the Leiden University Medical Centre (LUMC) study site of the longitudinal TRACK-HD study[28], 27 manifest gene carriers in the early disease stages one or two (early HD)[32], 22 premanifest gene carriers (prior to disease onset) and 25 healthy controls underwent 3T MRI scanning including an asymmetric spin echo sequence and functional assessment.

Inclusion criteria for the early HD group were a positive genetic test for the HTT gene with 40 or more CAG repeats, the presence of motor disturbances quantified by more than five points on the Unified Huntington's Disease Rating Scale – motor score (UHDRS-TMS), and a minimum Total Functional Capacity (TFC) score of seven points[32]. Inclusion criteria for premanifest gene carriers consisted of 40 or more CAG repeats, and the absence of motor disturbances with five or less points on the UHDRS-TMS. A burden of pathology score greater than 250[33] was required. Age- and gender-matched gene-negative relatives of HD gene carriers were included as healthy controls. Level of education in accordance to the International Standard Classification of Education (ISCED) was recorded. The study was approved by the Medical Ethical Committee and all participants gave informed consent.

MRI protocol

An MRI protocol including high-resolution 3D T_1-weighted and asymmetric spin echo (ASE) sequences was applied using a 3 Tesla whole body scanner (Achieva, Philips Healthcare, Best, The Netherlands) with an eight channel receive array head coil. Participants were positioned carefully with the application of strapping or cushioning where needed, to reduce the potential occurrence of involuntary head movement.

A 9.5 minute isotropic 1 mm^3 3D T_1-weighted scan was acquired with the following parameters: repetition time (TR)/ echo time (TE) = 7.7 ms/3.5 ms, field-of-view (FOV) = 24x24x16.4 cm^3. A T_2-weighted image (turbo spin echo) was acquired with the same volumetric spatial resolutions as the T_1-weighted images, with TE = 250 ms and TR = 2500 ms, also with a duration of 9.5 minutes. The T_2-weighted image for this study was only used to exclude any possible comorbidity. An 8 minute ASE sequence was implemented with the following scan parameters: TR/TE/flip angle = 1005 ms/38 ms/90°. The FOV was 22x19x7cm^3 with a voxel size of 1.9x1.7x2mm^3 for 18 slices with an interslice gap of 2 mm, positioned through the basal ganglia and an acquisition bandwidth of 290 Hz. The position of the refocusing radiofrequency pulse was shifted from its original position towards the excitation radiofrequency pulse by several time shifts = 0, 2.3, 6.9, 11.5 and 13.8 ms, thus varying the sensitivity of the sequence to magnetic field variations.

Post-processing of MRI images

Magnetic field correlation

Prior to post-processing all images were screened for artifacts and clinical abnormalities by a clinical neuroradiologist from the radiology department of the LUMC. Furthermore structural images were subjected to external quality control by a contract research organisation (IXICO Ltd, London, UK). ASE images were fitted to a theoretical model relating the signal decay to the homogeneity of the magnetic field[24]. The resulting MFC maps display the amount of magnetic field inhomogeneities present for each voxel. Higher MFC values correspond to a more inhomogeneous magnetic field. A correction was applied to the MFC maps to account for the contributions of macroscopic magnetic field inhomogeneities[21] using the non shifted image and the first asymmetric echo image of 2.3 ms. These macroscopic field inhomogeneities arising from, for example, the cavernous sinus and the skull are unrelated to iron content. The contributions from such areas were corrected to retain the underlying microscopic variations, such as those caused by iron, in the magnetic field in the remaining brain tissue.

Image Segmentation

Segmentation of the accumbens nucleus, amygdala, caudate nucleus, hippocampus, globus pallidus, putamen and thalamus was performed on the T_1-weighted scans using the FIRST tool[34] from FMRIB's Software Library (FSL, Oxford). Based on these segmentations, the absolute volume of each structure was calculated with FSLstats (FSL, Oxford), where the resulting value represents the total bi-lateral volume of a single structure. The volumetric analysis procedure, including a correction for intracranial volume, was identical to that described previously[27] making use of the FSL tools (FSL oxford). The segmentation masks were registered to the MFC maps using the T_1-weighted scans and the quality of the registration was visually inspected. Average MFC values were calculated for each segmented bilateral structure.

Statistics

To examine differences in MFC and volume between the groups, one-way Multivariate Analyses of Covariance (ANCOVA) were performed with the MFC value, or volumetric value (corrected for intracranial volume), of each subcortical structure as the outcome variable, while controlling for age and gender. The *p* value after post-hoc Bonferroni correction was considered significant at $p<0.05$.

To determine the independent potential for MFC value as a marker of disease state in HD, again only gene carriers were examined (premanifest+early HD, n=49). Logistic regression analysis was performed with disease state (premanifest vs. early HD) as the variable to be predicted. Age, gender, CAG repeat length, MFC value and volume of the relevant subcortical structures were included as predictor variables[19;35]. These were entered in one block (ENTER method) during analysis. All statistical analyses were performed with the

SPSS 17.0 package (SPSS Inc., Chicago, USA).

Subsequently, two analyses were performed to investigate the potential correlation between MFC values in any affected regions and volume changes in all gene carriers (premanifest + early HD). First, to investigate the direct relationship between MFC value and volume of the individual subcortical structures, Pearson's partial correlation analysis was performed, whilst controlling for the same covariates as in the logistic regression, namely age, gender and CAG repeat length. Secondly, to test for the potential influence of the interaction term (MFC value*volume) between MFC value and volume on disease state (premanifest or early HD), a general linear model univariate analysis of variance was performed.

To understand the potential relationship between iron levels and clinical measures, Pearson's partial correlation analysis was performed between iron in regions showing aberrant levels and clinical measures while controlling for age, gender and CAG repeat length. This was performed in the gene carrier group for the Unified Huntington's Disease Rating Scale – Total Motor Score (UHDRS), the Unified Huntington's Disease Rating Scale - Total functional Capacity measure (TFC), the number of correct answers on the Symbol Digit Modalities Test (SDMT), the number of correct answer on the Stroop word reading test (SWR) and the Beck's Depression Inventory 2nd Edition (BDI-II). For the premanifest gene carriers only an additional analysis was performed to understand any relationship between iron levels and the number of years to predicted disease onset, calculated according to the method by Langbehn *et al*. (2004)[35]. Pearson correlation was applied without covariates, as it is not appropriate to include covariates that are used in the prediction of expected disease onset. The *p* value was Bonferroni corrected for multiple comparisons.

Results

MFC value

No significant group differences were found for age, gender or education levels between controls, premanifest gene carriers, and early HD (table 1). The early HD group demonstrated lower scores on the TFC and higher total scores on the UHDRS ($p<0.001$) compared to the healthy control group and premanifest gene carriers.

Typical examples of the brain structure segmentations (figure 1a) and MFC maps in a healthy control (figure 1b), a premanifest gene carrier (figure 1c) and an early manifest patient (figure 1d) are shown in figure 1. This figure demonstrates the spatial distribution of the magnetic field inhomogeneities, with the highest values visible in the caudate nucleus, putamen, and globus pallidus. Higher MFC values were observed in the early HD group: the MFC group averages can be found in table 2 and are displayed in figure

2. The MFC values in the caudate nucleus and putamen of HD patients were found to be significantly higher than in healthy controls (p = 0.03 and p = 0.003, respectively). No significant differences were found between premanifest gene carriers and controls. No other nuclei showed differences either between early HD patients and controls, or between premanifest gene carriers and controls.

Table 1. Demographic information of controls, premanifest gene carriers, and early Huntington's disease

		Healthy Controls	Premanifest Gene Carriers	Early Manifest Patients
N		25	22	27
Gender	Female/Male	13/12	13/9	19/8
Age	Mean yrs ± SD	50.3 ± 8.3	45.6 ± 8.5	50.0 ± 9.9
	Range (min – max)	36 - 66	27 - 62	30 - 64
Education level	Mean ISCED level ± SD	3.4 ± 1.1	3.8 ± 1.1	3.2 ± 1.3
UHDRS	Mean total score ± SD	2.1 ± 1.7	2.6 ± 1.4	25.2 ± 15.4*
TFC	Mean ± SD; Range: 0-13	12.9 ± 0.2	12.5 ± 0.8	9.8 ± 2.8*

N = number of participants, SD = Standard Deviation, ISCED = International Standard Classification of Education (range 0-6), UHDRS = Unified Huntington's Disease Rating Scale – Total Motor Score, TFC = Total Functional Capacity, * Significantly different from both healthy controls and premanifest HD at p<0.001.

Figure 1. Typical example of magnitude images

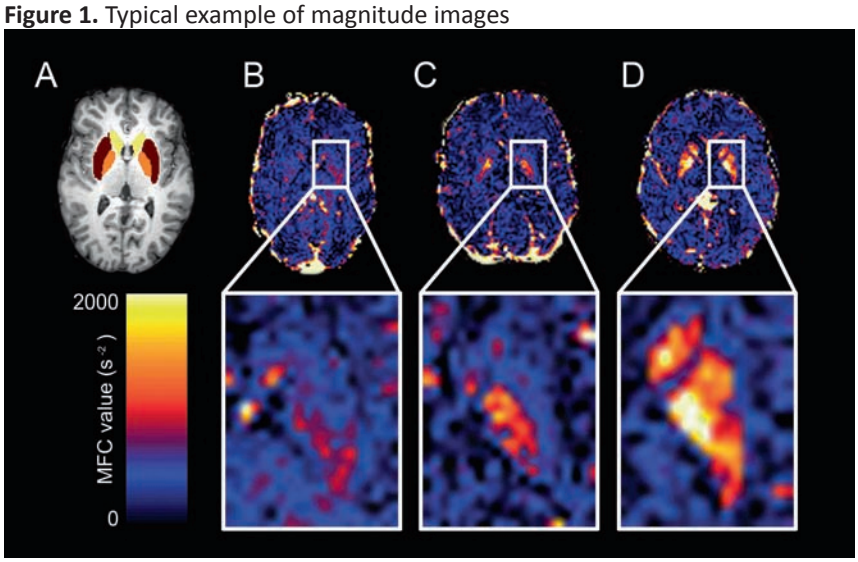

A) Magnitude image showing segmentation of caudate nucleus (yellow), putamen (brown) and globus pallidus (orange). The corresponding MFC maps for a healthy control (B), premanifest gene carrier (C) and early Huntington's disease patient (D). High MFC values are found in the subcortical grey matter structures, known to correspond with high iron concentrations. Highest values are found in the early HD patient. The high MFC values found laterally near the tissue-skull interface are caused by macroscopic magnetic field inhomogeneities from the skull tissue interface that could not be properly corrected. The distance to the areas of interest is so large that no interference with measurements in the deep gray matter structures is expected.

Figure 2. Groups differences in MFC

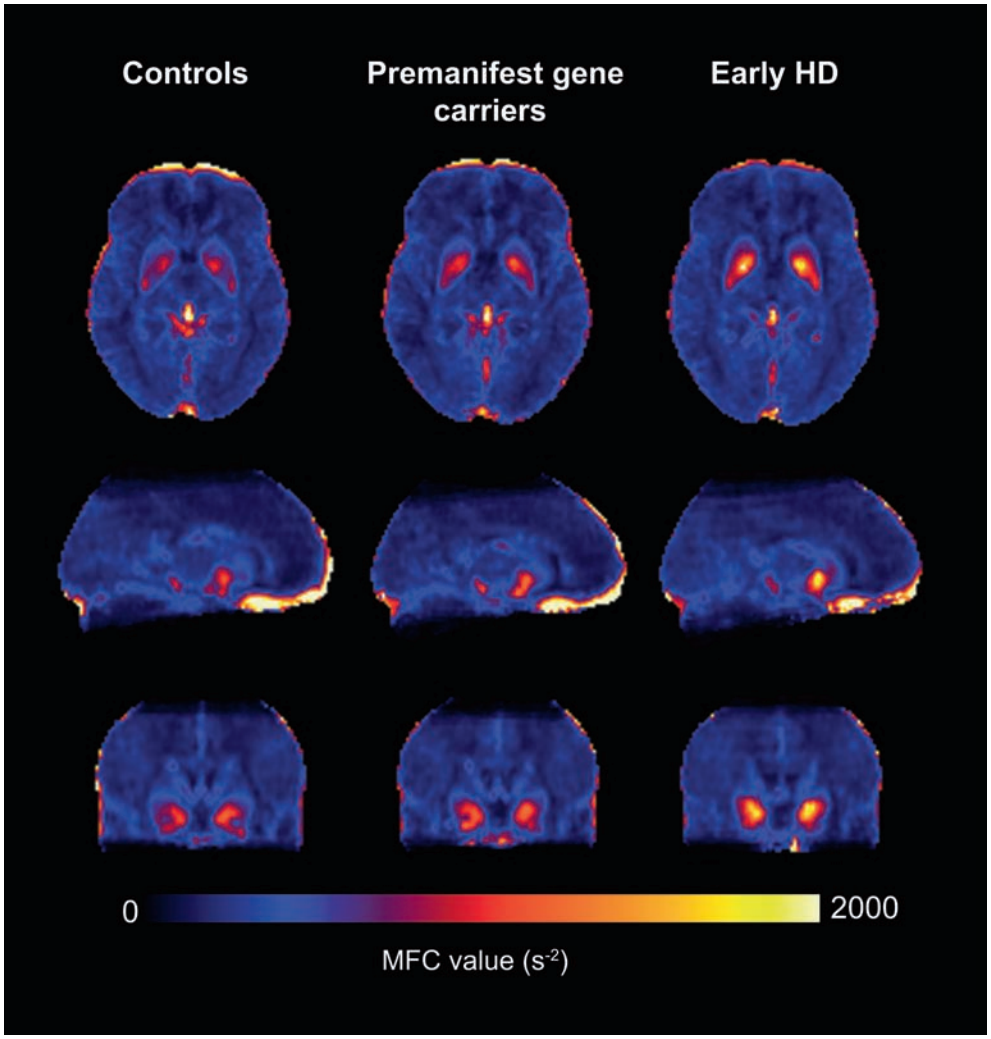

Figure 2: MFC group averages for controls, premanifest and manifest HD. All images were registered to standard space and averaged. The resulting average is a visual display of the values shown in table 2, however more localised information is present in this visual display. High MFC values are found in the subcortical grey matter structures, known to correspond with high iron concentrations.

Volume

The volumes of the caudate nucleus and putamen were smaller in early HD patients compared to premanifest gene carriers and controls, and also smaller in premanifest gene carriers as compared to controls (all $p<0.0001$). Smaller volumes of the accumbens nucleus ($p<0.0001$), globus pallidus ($p<0.0001$) and thalamus ($p=0.001$) were also found in early HD as compared to healthy controls only (table 2).

Table 2. Average MFC values and subcortical grey matter volumes per subcortical nucleus per study group

	Mean MFC(s^{-2})	SD	Volume (ml)	SD
Accumbens nucleus				
Control group	385.6	101.2	1.10	.25
Premanifest	343.2	93.7	**.98***	.19
Early HD	450.3	219.1	**.76**§**	.17
Amygdala				
Control group	446.6	122.0	2.54	.44
Premanifest	419.0	108.6	2.46	.45
Early HD	412.2	111.9	2.29	.42
Caudate nucleus				
Control group	398.6	55.0	6.96	.91
Premanifest	372.4	76.8	**5.86****	.72
Early HD	478.1*§§	153.1	**4.72**§§**	.76
Hippocampus				
Control group	452.0	102.8	7.91	.82
Premanifest	400.0	59.8	7.80	.80
Early HD	409.6	102.2	7.21	.86
Globus pallidus				
Control group	643.7	120.8	3.54	.42
Premanifest	715.3	215.2	3.27	.47
Early HD	807.4	368.9	**2.67**§§**	.44
Putamen				
Control group	481.8	120.6	4.83	.71
Premanifest	491.8	154.0	**4.14****	.50
Early HD	**632.1**§**	190.6	**3.28**§§**	.50
Thalamus				
Control group	388.4	60.3	15.23	1.45
Premanifest	377.8	92.9	14.80	1.39
Early HD	373.6	82.1	**13.67****	1.39

MFC values represent average value in s^{-2}. Volumetric analysis performed with correction for intercranial volume, volumes reported represent absolute total volume of each left and right nucleus.

* Significantly different from healthy controls (p<0.05)

** Significantly different from healthy controls (p<0.005)

§ Significantly different from premanifest gene carriers (p<0.05)

§§ Significantly different from premanifest gene carriers (p<0.005)

Predicting disease state

Logistic regression was performed to assess the predictive quality of subcortical MFC values of the caudate nucleus and putamen to disease state in all gene carriers (premanifest or early HD) as shown in table 3. The MFC values and volumes of the caudate nucleus, and putamen were significant predictors of disease state. In contrast, age, gender and CAG repeat length were not significant contributors to the prediction of disease state. Figure 3 shows the relationship between volume and MFC value for the caudate nucleus and putamen. In assessing further the independence of these two significant predictors the Pearson's partial correlation showed that the MFC value and volume were not related

to one another in the caudate nucleus (r=-0.105, *p*=0.486) or putamen (r=-0.132, *p*=0.382) in gene carriers (premanifest + early HD). The univariate analysis of variance assessing any potential interaction effect of MFC and volume on disease state also showed no interaction (caudate nucleus: *p*=0.916; putamen: *p*=0.992).

Table 3. Logistic regression model for predicting disease state (premanifest vs. early manifest) in all gene carrying participants

	Total model			Level of statistical significance (p value)	
	χ^2	DF	p	MFC value	Volume
Caudate nucleus	33.3	5	<0.0005	0.02	0.01
Putamen	40	5	<0.0005	0.04	0.01

Table shows only those predictors that significantly contributed to the model. MFC values represent average value per subcortical nucleus. DF = degrees of freedom. Volumes included are total volume of left and right nucleus per subcortical structure.

Relationship to clinical measures

The relationship between clinical measures and iron levels in the caudate nucleus and putamen was examined for both gene carriers groups. No relationship was found between UHDRS total motor score, TFC, SDMT, SWR or BDI-II and iron levels in the putamen or caudate nucleus. For the premanifest group only correlation no significant relationship between predicted years to onset and iron in the caudate nucleus or putamen was shown. Individual iron levels versus a measure of disease load, namely burden of disease pathology[33], are displayed for individual gene carriers in figure 4.

Figure 3: Individual MFC values set out against volumetric data for (A) caudate nucleus and (B) putamen.

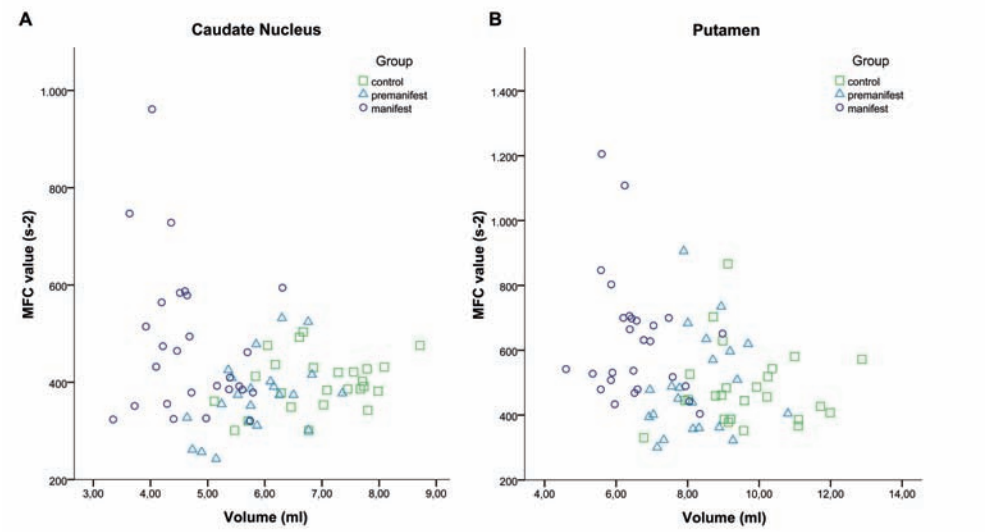

Figure 4: Burden of disease pathology scores ((CAG - 35.5) * age) versus MFC values for all gene carriers (premanifest + manifest) in the caudate nucleus and putamen.

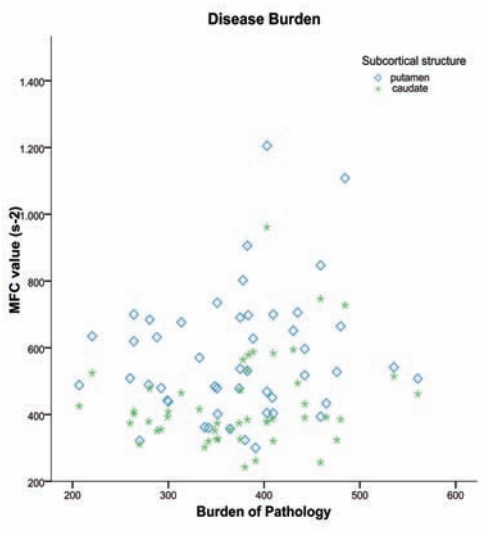

Discussion

This study's main findings show increased levels of iron, as demonstrated by higher MFC values, in caudate nucleus and putamen in patients with early HD. MFC values were not significantly different to controls in premanifest gene carriers. For clarity and consistency with other studies, we will refer to changes in the measured iron-dependent quantity, namely MFC values, as changes in iron[11;16;36]. The iron levels in the putamen and caudate nucleus are not related to the volume of these structures. Furthermore, iron levels appear to predict the disease state (premanifest or early manifest) of HD gene carriers.

In early HD the caudate nucleus and putamen show significantly higher MFC values. This is in line with in vivo[11;19] and ex vivo[5;18] findings. The relative MFC values in the healthy controls correspond to ex-vivo-determined levels of iron, whereby the globus pallidus showed highest values for all participant groups, which is in agreement with previous studies of both aging and neurodegeneration[36-38].

No significant differences in iron were observed between premanifest gene carriers and healthy controls. The only other report in premanifest gene carriers found elevated iron in the globus pallidus[29]. However, this report was based on a group with less stringent inclusion criteria of individuals, namely without overt motor signs as opposed to a UHDRS cut-off point of 5. The correlation which Jurgens *et al*. (2010) found between the number of hypointense pixels and total motor score, demonstrates that all of the participants with higher iron levels would have been classified as having early manifest HD under our criteria[29]. It is certainly possible that the iron levels are not high enough for MFC, or any other existing imaging techniques, to pick up small changes in premanifest gene carriers, or that abnormal iron depositions do not occur until later in the disease process. The volumetric decreases of the caudate nucleus and putamen in premanifest gene carriers found in this present study are in line with previous reports[25-27].

This study has demonstrated that the individual iron content of the caudate nucleus and putamen independently predicts disease state in gene carriers (premanifest versus early manifest), also when taking into consideration the predictive value of other commonly related factors, such as volume, CAG repeat length or age. Furthermore the iron content in the putamen and caudate nucleus is not directly related to the volume of these structures, and there is no interaction effect present that explains disease state. Therefore, our results indicate that volumetric decrease and iron increase are two independent processes in HD, with iron accumulation not occurring as a direct result of volume decrease (Figure 4). This is an important finding as it reiterates the need for increasing our understanding of the pathophysiological processes related to iron in HD. When considering this conclusion it is important to exclude the possibility of epiphenomenonological results, especially in early

HD. We addressed this by accounting for those factors most commonly found to explain the variance between premanifest and manifest gene carriers[33;35]. We propose that iron levels may be regarded as a marker of disease state, as iron does not differentiate those prior to disease onset from controls, but does distinguish between premanifest gene carriers and those in the earliest stages of HD. Reproduction and longitudinal evaluation of potential iron accumulation may demonstrate the capacity to predict symptom progression or, as previously suggested, the age of disease onset[39].

Iron content in early HD was not found to be higher than in controls in the amygdala, hippocampus, nucleus accumbens or thalamus. This both replicates and also adds to previous findings in which no differences were found in the hippocampus and thalamus[19]. We have measured a pattern of elevated iron in early HD that could be toxic or an accelerated process of normal aging. However, oxidative stress related mechanisms, as a result of higher free radicals cannot be excluded[40]. It may be that iron depositions primarily affect nuclei that consist of the same types of cells, such as the medium spiny neurons common to the putamen and caudate nucleus, or as demonstrated in HD patients and mice, the microglia[4]. Many hypotheses on the role of iron in neurodegeneration have been formulated but the exact mechanisms remains unclear[12;41;42].

Globus pallidus iron depositions showed an increase in the early HD group as compared to controls: however, this was not statistically significant. This may be related to the sequence parameters, and not due to an intrinsic absence of higher iron levels, especially as another study in manifest HD[19] found higher iron in the globus pallidus. The chosen ASE parameters could be suboptimal for measurements in areas of very high iron concentration as a result of the pronounced signal reduction. As a result a higher standard deviation can be expected in the MFC maps within the globus pallidus, which was indeed the case. Future research at ultra high field strength (7 Tesla and above) could increase the sensitivity of the MFC method.

We believe that the technique used in our study is a more direct measure of iron than conventional T_2-, T_2^*- and SWI based methods that have been used extensively to study the distribution of iron in the brain[8;9;14], due primarily to the robustness with respect to any altered water concentrations. In the study by Bartzokis *et al*. (2007) T_2 relaxation values were obtained by scanning patients at two different field strengths and significant differences were found in iron concentration of the putamen, globus pallidus, and caudate nucleus in manifest HD patients[19]. This is comparable to the results of our study. Vymazal *et al*. (2007) measured T_2 relaxation values at a single field strength and found changes in the globus pallidus and white matter only in HD patients[16]. The discrepancy between these and our results can potentially be explained by the sensitivity of T_2 measurements to water content, which is thought to change during disease progression due to, for example,

breakdown of the structural integrity of myelin[9;15;19]. Although we cannot definitively exclude all potential sources of magnetic field variation[43], we believe that based on ex-vivo studies[4;14] the changes observed in our and previous studies are related primarily to increased iron. An advantage of MFC measurements is that the macroscopic component of the field inhomogeneities can be separated from the microscopic components, which is a confounding factor for T_2^* based techniques.

A possible limitation could be the influence of other sources of magnetic field variation, such as the cavernous sinus or skull. However all possible steps were taken to prevent this influence. After correction a remainder of macroscopic field variations is still present located laterally near skull-tissue interface and around large vessels. However, upon visual inspection, the macroscopic contribution of these regions around the basal ganglia are adequately corrected.

In conclusion, we have demonstrated that patients with early HD have higher magnetic field inhomogeneities in the caudate nucleus and putamen. This is not found in premanifest gene carriers. The iron content of the caudate nucleus, putamen seems to independently predicts disease state in HD gene carriers. Futhermore, we have demonstrated that increased iron accumulation is an independent disease process not related to structural atrophy.

References

1. Roos RAC, Pruyt JFM, Devries J, et al. Neuronal Distribution in the Putamen in Huntingtons-Disease. *Journal of Neurology Neurosurgery and Psychiatry* 1985;48:422-25
2. Roos RAC, Bots GTAM. Nuclear-Membrane Indentations in Huntingtons-Chorea. *Journal of the Neurological Sciences* 1983;61:37-47
3. Vonsattel JPG, DiFiglia M. Huntington disease. *Journal of Neuropathology and Experimental Neurology* 1998;57:369-84
4. Simmons DA, Casale M, Alcon B, et al. Ferritin accumulation in dystrophic microglia is an early event in the development of Huntington's disease. *Glia* 2007;55:1074-84
5. Dexter DT, Carayon A, Javoyagid F, et al. Alterations in the Levels of Iron, Ferritin and Other Trace-Metals in Parkinsons-Disease and Other Neurodegenerative Diseases Affecting the Basal Ganglia. *Brain* 1991;114:1953-75
6. Haacke EM, Chengb NYC, House MJ, et al. Imaging iron stores in the brain using magnetic resonance imaging. *Magnetic Resonance Imaging* 2005;23:1-25
7. Aquino D, Bizzi A, Grisoli M, et al. Age-related iron deposition in the basal ganglia: quantitative analysis in healthy subjects. *Radiology* 2009;252:165-72
8. Haacke EM, Miao YW, Liu MJ, et al. Correlation of Putative Iron Content as Represented by Changes in R2* and Phase With Age in Deep Gray Matter of Healthy Adults. *Journal of Magnetic Resonance Imaging* 2010;32:561-76
9. Gelman N, Gorell JM, Barker PB, et al. MR imaging of human brain at 3.0 T: Preliminary report on transverse relaxation rates and relation to estimated iron content. *Radiology* 1999;210:759-67
10. Xu X, Wang Q, Zhang M. Age, gender, and hemispheric differences in iron deposition in the human brain: An in vivo MRI study. *Neuroimage* 2008;40:35-42
11. Bartzokis G, Cummings J, Perlman S, et al. Increased basal ganglia iron levels in Huntington disease. *Arch Neurol* 1999;56:569-74
12. Brass SD, Chen NK, Mulkern RV, et al. Magnetic resonance imaging of iron deposition in neurological disorders. *Top Magn Reson Imaging* 2006;17:31-40
13. Graham JM, Paley MN, Grunewald RA, et al. Brain iron deposition in Parkinson's disease imaged using the PRIME magnetic resonance sequence. *Brain* 2000;123 Pt 12:2423-31
14. Schenck JF, Zimmerman EA. High-field magnetic resonance imaging of brain iron: birth of a biomarker? *NMR Biomed* 2004;17:433-45
15. Bartzokis G, Sultzer D, Lu PH, et al. Heterogeneous age-related breakdown of white matter structural integrity: implications for cortical "disconnection" in aging and Alzheimer's disease. *Neurobiol Aging* 2004;25:843-51
16. Vymazal J, Klempir J, Jech R, et al. MR relaxometry in Huntington's disease: correlation between imaging, genetic and clinical parameters. *J Neurol Sci* 2007;263:20-25
17. Haller S, Bartsch A, Nguyen D, et al. Cerebral microhemorrhage and iron deposition in mild cognitive impairment: susceptibility-weighted MR imaging assessment. *Radiology* 2010;257(3):764-73
18. Chen JC, Hardy PA, Kucharczyk W, et al. MR of human postmortem brain tissue: correlative study between T2 and assays of iron and ferritin in Parkinson and Huntington disease. *AJNR Am J Neuroradiol* 1993;14:275-81
19. Bartzokis G, Lu PH, Tishler TA, et al. Myelin breakdown and iron changes in Huntington's disease: Pathogenesis and treatment implications. *Neurochemical Research* 2007;32:1655-64
20. Haacke EM, Xu Y, Cheng YC, et al. Susceptibility weighted imaging (SWI). *Magn Reson Med* 2004;52:612-18
21. Jensen JH, Szulc K, Hu C, et al. Magnetic field correlation as a measure of iron-generated magnetic field inhomogeneities in the brain. *Magn Reson Med* 2009;61:481-85
22. Raz E, Jensen JH, Ge Y, et al. Brain Iron Quantification in Mild Traumatic Brain Injury: A Magnetic Field Correlation Study. *AJNR Am J Neuroradiol* 2011;
23. Ge Y, Jensen JH, Lu H, et al. Quantitative assessment of iron accumulation in the deep gray matter of multiple sclerosis by magnetic field correlation imaging. *AJNR Am J Neuroradiol* 2007;28(9):1639-44

24. Jensen JH, Chandra R, Ramani A, et al. Magnetic field correlation imaging. *Magn Reson Med* 2006;55:1350-61
25. Paulsen JS, Magnotta VA, Mikos AE, et al. Brain structure in preclinical Huntington's disease. *Biol Psychiatry* 2006;59:57-63
26. Aylward EH, Li Q, Stine OC, et al. Longitudinal change in basal ganglia volume in patients with Huntington's disease. *Neurology* 1997;48:394-99
27. van den Bogaard SJ, Dumas EM, Acharya TP, et al. Early atrophy of pallidum and accumbens nucleus in Huntington's disease. *J Neurol* 2010;258:412-20
28. Tabrizi SJ, Langbehn DR, Leavitt BR, et al. Biological and clinical manifestations of Huntington's disease in the longitudinal TRACK-HD study: cross-sectional analysis of baseline data. *Lancet Neurol* 2009;8:791-801
29. Jurgens CK, Jasinschi R, Ekin A, et al. MRI T2 Hypointensities in basal ganglia of premanifest Huntington's disease. *PLoS Curr* 2010;2: pii: RRN1173
30. Stankiewicz JM, Brass SD. Role of iron in neurotoxicity: a cause for concern in the elderly? *Current Opinion in Clinical Nutrition and Metabolic Care* 2009;12:22-29
31. Aylward EH, Codori AM, Rosenblatt A, et al. Rate of caudate atrophy in presymptomatic and symptomatic stages of Huntington's disease. *Mov Disord* 2000;15:552-60
32. Shoulson I, Fahn S. Huntington disease: clinical care and evaluation. *Neurology* 1979;29:1-3
33. Penney JB, Vonsattel JP, MacDonald ME, et al. CAG repeat number governs the development rate of pathology in Huntington's disease. *Annals of Neurology* 1997;41:689-92
34. Patenaude B, Smith SM, Kennedy DN, et al. A Bayesian model of shape and appearance for subcortical brain segmentation. *Neuroimage* 2011;56:907-22
35. Langbehn DR, Brinkman RR, Falush D, et al. A new model for prediction of the age of onset and penetrance for Huntington's disease based on CAG length. *Clin Genet* 2004;65:267-77
36. Hallgren B, Sourander P. The Effect of Age on the Non-Haemin Iron in the Human Brain. *Journal of Neurochemistry* 1958;3:41-51
37. Bartzokis G, Tishler TA. MRI evaluation of basal ganglia ferritin iron and neurotoxicity in Alzheimer's and Huntingon's disease. *Cellular and Molecular Biology* 2000;46:821-33
38. Drayer B, Burger P, Darwin R, et al. MRI of brain iron. *AJR Am J Roentgenol* 1986;147:103-10
39. Bartzokis G, Tishler TA, Shin IS, et al. Brain ferritin iron as a risk factor for age at onset in neurodegenerative diseases. *Ann N Y Acad Sci* 2004;1012:224-36
40. Ischiropoulos H, Beckman JS. Oxidative stress and nitration in neurodegeneration: cause, effect, or association? *J Clin Invest* 2003;111:163-69
41. Berg D, Youdim MB. Role of iron in neurodegenerative disorders. *Top Magn Reson Imaging* 2006;17:5-17
42. Zecca L, Youdim MBH, Riederer P, et al. Iron, brain ageing and neurodegenerative disorders. *Nature Reviews Neuroscience* 2004;5:863-73
43. Wu Z, Mittal S, Kish K, et al. Identification of calcification with MRI using susceptibility-weighted imaging: a case study. *J Magn Reson Imaging* 2009;29:177-82